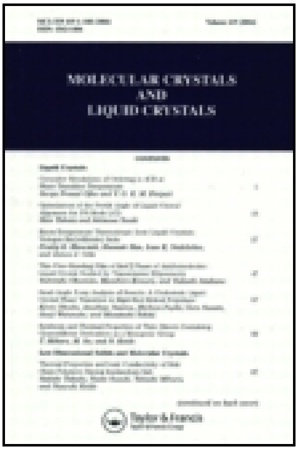

Molecular Crystals and Liquid Crystals Science and Technology. Section A. Molecular Crystals and Liquid Crystals

Publication details, including instructions for authors and subscription information:
http://www.tandfonline.com/loi/gmcl19

EVALUATION OF ELASTIC PROPERTIES IN NEMATIC LIQUID CRYSTAL USING ELASTIC WAVE PROPAGATION

Masaru Inoue [a], Hiroshi Moritake [b], Katsumi Yoshino [a] & Kohji Toda [b]

[a] Department of Electronic Engineering, Graduate School of Engineering, Osaka University, Yamadaoka, Suita, 565-0871, Japan

[b] Department of Electrical and Electronic Engineering, National Defense Academy, Hashirimizu, Yokosuka, 239-8686, Japan

Version of record first published: 24 Sep 2006

Mol. Cryst. and Liq. Cryst., 2001, Vol. 366, pp. 173-181
Reprints available directly from the publisher
Photocopying permitted by license only

Evaluation of Elastic Properties in Nematic Liquid Crystal using Elastic Wave Propagation

MASARU INOUE[a], HIROSHI MORITAKE[b], KATSUMI YOSHINO[a] and KOHJI TODA[b]

[a]*Department of Electronic Engineering, Graduate School of Engineering, Osaka University, Yamadaoka, Suita 565–0871, Japan and* [b]*Department of Electrical and Electronic Engineering, National Defense Academy, Hashirimizu, Yokosuka 239–8686, Japan*

An interaction between an elastic wave and a liquid crystal is investigated from the view point of evaluation of the elastic properties of the liquid crystal. A periodical stripe domain pattern is induced by an interaction between the elastic wave and the nematic liquid crystal, the pattern is observed by a polarizing microscope. In the numerical analysis of elastic wave propagation in a nematic liquid crystal cell, the 0th mode depends on the liquid crystal properties, on the other hand the 1st mode is influenced predominantly by the properties of two sheets of glasses composing the cell. The 0th and 1st mode phase velocities are estimated from the periodic length of the stripe domain pattern. The 0th mode phase velocity in the nematic liquid crystal cell strongly depends on the cell layer thickness. The phase velocity obtained from the observed result is in good agreement with the numerical analysis result.

Keywords: elastic wave propagation; nematic liquid crystal; velocity evaluation; trilayer structure; interdigital transducer (IDT)

INTRODUCTION

Recent works on elastic wave propagation at a solid/liquid interface have covered the viewpoints of not only physics but also engineering application, including liquid phase sensing [1-3]. The elastic wave sensing devices detect the fractional velocity change [4,5] or the propagation loss [6], which have some possibilities of measuring dielectric constant [7], viscosity [8], sound velocity [9], and chemical quantity [10]. The interaction between an elastic wave propagation and a liquid crystal has been reported [11,12]. The step for detailed evaluation of elastic properties of liquid crystal has not been reached.

In this study, the phase velocity of the elastic wave propagating in the nematic liquid crystal is analyzed numerically and experimentally. The numerical analysis is carried out in a trilayer structure containing the liquid crystal sandwiched between two glass plates. The phase velocity of the elastic wave propagating in a typical nematic liquid crystal (4'-methoxybenzylidene-4-n-butylaniline: MBBA) is evaluated in the relation with the observation of the periodic length of the stripe domain induced by the elastic wave propagation.

NUMERICAL ANALYSIS RESULTS

In this section, a theoretical description of elastic wave propagation in a fluid sandwiched between two identical solid plates is given. Figure 1 shows a coordinate system for numerical analysis in this study. The elastic wave propagation is along X axis and the liquid crystal cell has the solid-fluid interfaces at $Z = \pm d/2$. A rigorous treatment of the hydrodynamical problem of the liquid crystal is extremely difficult. In the case of the elastic wave propagation in the nematic liquid crystal, the liquid-crystalline medium is regarded as a simple viscous isotropic fluid [11]. The material constants used for the numerical calculation and the experiment are listed in Table 1, where η is the viscosity and V_L is the longitudinal wave velocity in MBBA.

TABLE 1 Material constants of glass plate and liquid crystal.

property	glass plate	LC (MBBA)	units
c_{11}	8.63		$\times10^{10}$[N/m^2]
c_{12}	3.36		$\times10^{10}$[N/m^2]
c_{44}	2.64		$\times10^{10}$[N/m^2]
ϵ	5.60		
ρ	2760	1043	kg/m^3
η		0.02 to 0.07	Pa.s
V_L		1550 (30°C)	m/s

Figure 2 shows the phase velocity dispersion curves of the elastic waves propagating in the liquid crystal cell as a function of fd (MHz·mm). Multiple modes are recognizable, the 0th and 1st modes exist over the entire fd range. The phase velocity of the 0th mode increases with fd value, and reaches a constant value corresponding to the longitudinal wave velocity of the liquid crystal, 1550 m/s. The phase velocity of the 1st mode at $fd = 0$ equal to the surface wave velocity on the glass plate. Other higher-order modes appear critically near the shear wave velocity in the glass plate.

Figure 3 shows the calculated fractional phase velocity changes of the lowest three modes propagating in the liquid crystal cell layer, as a function of the longitudinal wave velocity in the liquid crystal over the range of

1250 m/s to 1550 m/s, under the condition that the frequency is 10MHz, and the density and the viscosity of the liquid crystal are kept constant, an listed in Table 1. The 0th mode phase velocity strongly depends on the longitudinal wave velocity in the liquid crystal.

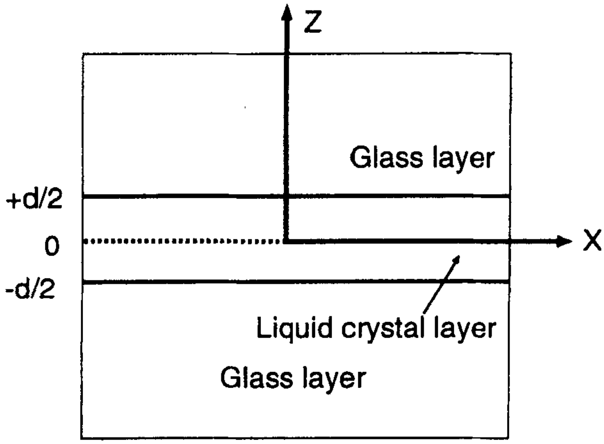

FIGURE 1 Coordinate system for numerical analysis of elastic wave propagation.

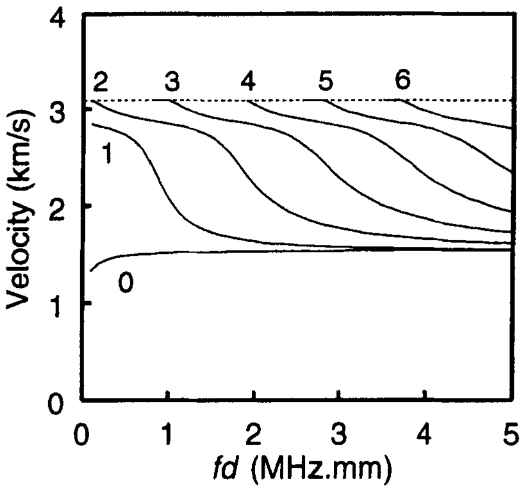

FIGURE 2 Velocity dispersion curves of elastic wave modes in nematic liquid crystal cell.

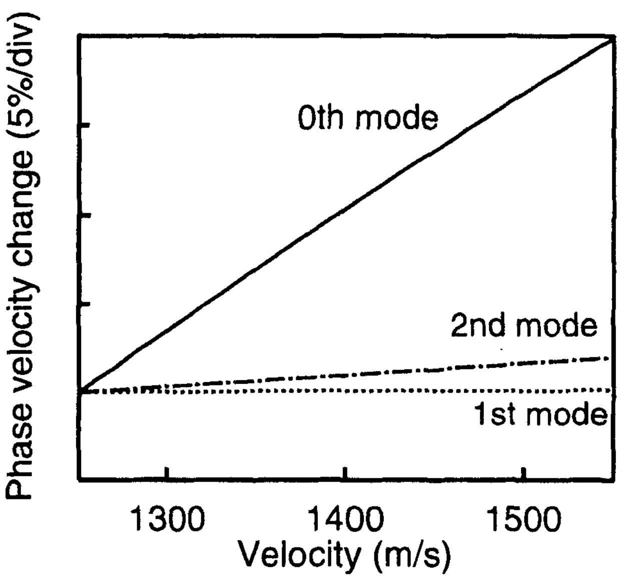

FIGURE 3 Calculated dependences of fractional velocity change on longitudinal velocity in liquid crystal.

EXPERIMENTAL RESULTS

A schematic construction of the device prepared for the present study is shown in Fig. 4. Two interdigital transducers (IDTs) are mounted on a 230-μm-thick piezoelectric ceramic thin plate (TDK, 101A) cemented to a 1.1-mm-thick glass plate (Corning, 7059) with epoxy resin. Each of the IDTs has an interdigital periodicity of 500μm and six electrode finger pairs. The nematic liquid crystal (MBBA) is sandwiched between two glass plates whose surface were coated with polyimide (JSR, AL1254) and rubbed unidirectionally. The thickness of the liquid crystal layer was adjusted by a PET film, as 25μm and 12μm. MBBA shows the nematic phase at room temperature and all of the experiments were performed at about 25°C.

Figure 5 shows the measured frequency dependences of the insertion losses of the device with (rigid line) and without (dotted line) the liquid crystal. In this case, the thickness of the liquid crystal layer is 25 μm. The observed peaks of the insertion loss curves correspond to the respective center frequency of each mode of the elastic wave propagating in a piezoelectric ceramic thin plate and in a layered cell structure.

Polarizing microscopic observation of the liquid crystal cell was executed under the existence of the elastic wave excited by the IDT. A typical stripe domain pattern was observed, as shown in Fig. 6, in the case of the application of a 7.0 MHz CW signal to the IDT. The longer periodic domain perpendicular to the elastic wave propagation and the shorter periodic domain existing in the longer periodic domain are observed. In this study, the longer periodic domain is focused and discussed. These two types of domains appear when the acoustic power is beyond a threshold level. With further increase of the acoustic power, these patterns are disturbed by the vortex motion of the molecules of the nematic liquid crystal.

Figure 7 shows the observed frequency dependences of the domain periodicity in the nematic liquid crystal. White and black circles correspond to the results for the 25 μm and 12 μm-thick liquid crystal layers, respectively. The period of the domain depends on the thickness of the liquid crystal layer and the frequency of the elastic wave. The period of stripe domain decreases with an increase of the carrier frequency of the elastic wave. It is considered that the domain formation is the result of molecular orientation in the nematic liquid crystal, induced by the elastic wave propagation.

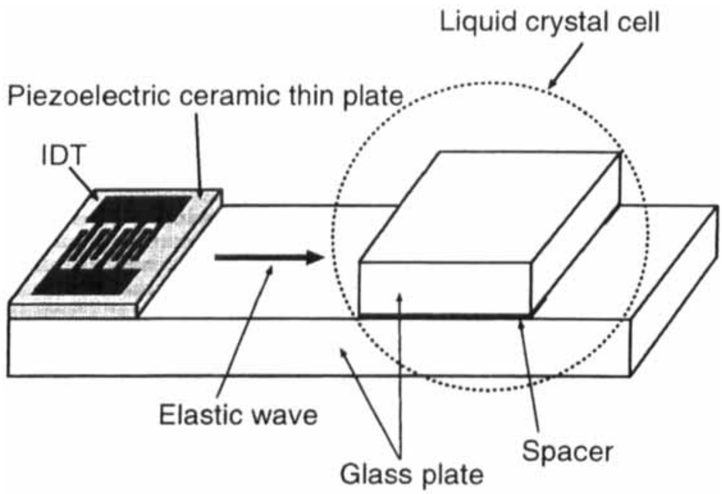

FIGURE 4 Schematic construction of device for experiment.

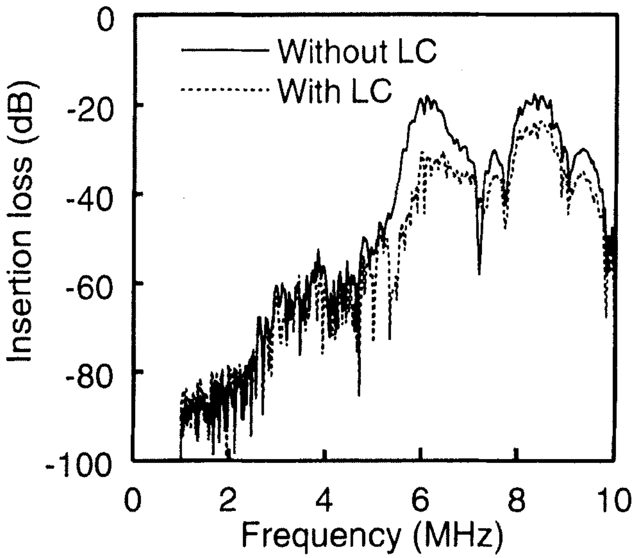

FIGURE 5 Measured frequency dependences of insertion loss of device with 500μm interdigital periodicity: rigid and dotted lines are for device without and with liquid crystal (MBBA), respectively.

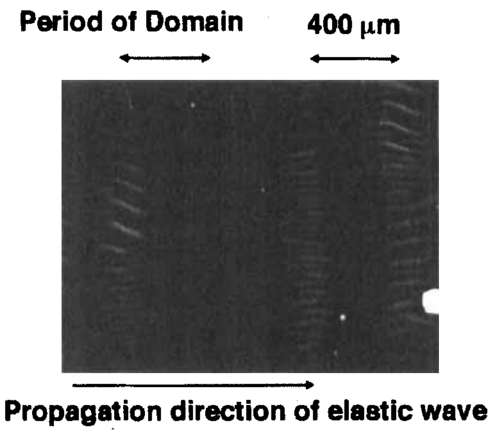

FIGURE 6 Observed periodic domain pattern induced by elastic wave propagation in nematic liquid crystal cell.

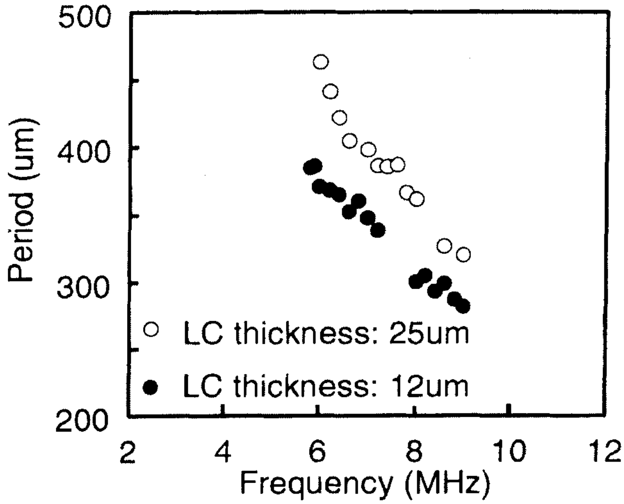

FIGURE 7 Frequency dependences of periodic length of domain pattern induced in nematic liquid crystal cell.

VELOCITY EVALUATION

From the velocity curves in Fig. 2, 0th, 1st and 2nd mode can propagate in the sandwiched nematic liquid crystal cell in the low frequency region. The periodic stripe domain is induced by a nonlinear interaction between several modes, which is known as acoustic streaming [11]. The interaction causes a vortex motion in the liquid crystal cell. As the result, the molecular orientation of liquid crystal is induced by its flow. The periodic length P is represented by the following relation [11]:

$$P = \frac{2\pi}{k_0 - k_1}. \tag{1}$$

where $k_i (i = 0, 1)$ is the wave number of each mode. In this study, P is the observed periodic domain length and k_1 is obtained from the 1st mode phase velocity in Fig. 2. As a result, the wave number k_0 is calculated using the above relation. The 0th mode phase velocity strongly depends on the longitudinal wave velocity in the nematic liquid crystal, as shown in Fig. 3. The 1st mode phase velocity in the nematic liquid crystal cell is also estimated through a similar procedure.

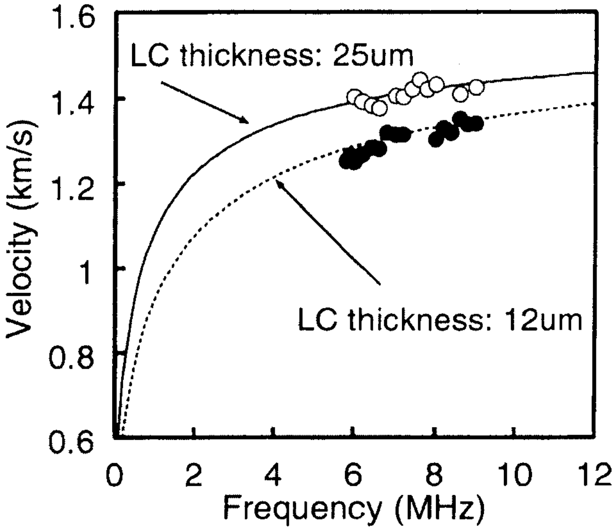

FIGURE 8 Comparison between numerical velocity curves (rigid line: LC thickness is 25μm, dotted line: LC thickness is 12μm) and evaluated data for 0th mode in MBBA (white circles: LC thickness is 25μm, black circles is 12μm).

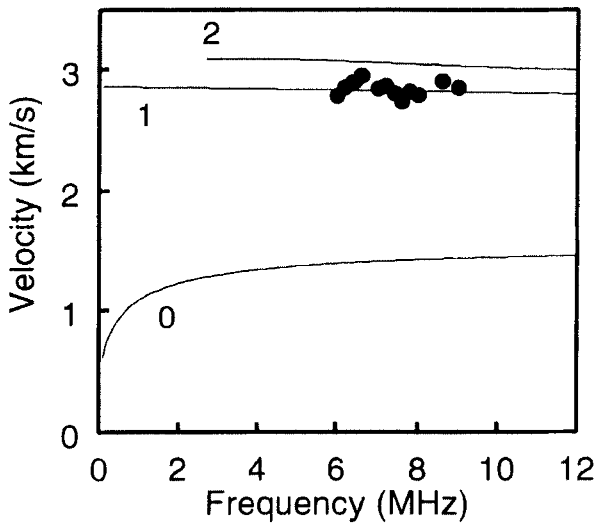

FIGURE 9 Comparison between numerical velocity curves (rigid line) and evaluated data for 1st mode in MBBA.

Figure 8 shows the comparison between the numerical result and the estimated results of the 0th mode phase velocity in the nematic liquid crystal (MBBA) cell. Rigid and broken lines indicate the 0th mode phase velocity curves from the numerical calculation in the cases of 25 μm and 12 μm-thick liquid crystal layers, respectively. White and black circles indicate the 0th mode phase velocity data obtained from the above relations in the cases of 25 μm and 12 μm-thick liquid crystal layers, respectively. It is obvious that the evaluated data are in good agreement with the numerical calculation results.

The numerical 1st mode phase velocity curve is compared with the experimentally obtained data, as shown in Fig. 9. The evaluated data has good consistency with numerical calculation results.

CONCLUSION

A periodic domain pattern excited by an elastic wave propagating in a sandwiched liquid crystal cell was related to the velocity dispersion curves. The phase velocity in the nematic liquid crystal cell is evaluated from the observed periodic length of the induced stripe domain. The present method of observing the periodic length of the stripe domain is promising for evaluating the phase velocity of the elastic wave propagating in a liquid crystal cell layer.

References

[1] S.W. Wenzel and R.M. White, *IEEE Trans. Elect. Dev.*, **35**, 735 (1988).
[2] R.M. White and S.W. Wenzel, *Appl. Phys. Lett.*, **52**, 1653 (1988).
[3] H. Moritake, K. Takahashi, K. Yoshino and K. Toda, *Jpn. J. Appl. Phys.* **35**, 5220 (1996).
[4] A. Sawaguchi and K. Toda, *Jpn. J. Appl. Phys.*, 3094 (1992).
[5] J.J. Caron, R.B. Haskell, P. Benoit and J.F. Vetelino, *IEEE Trans. Ultrason., Ferroelec., & Freq. Contr.*, **45**, 1393 (1998).
[6] J.O. Kim, *J. Acoust. Soc. Am.*, **91**, 3099 (1992).
[7] F. Josse, D.T. Haworth, U.R. Kelkar and Z.A. Shana, *Electron Lett.*, **26**834 (1990).
[8] A.J. Ricco and S.J. Martin, *Appl. Phys. Lett.*, **50**, 1474 (1987).
[9] A. Sawaguchi and K. Toda, *Jpn. J. Appl. Phys.*, **31**, 75 (1992).
[10] R.A. McGill, R. Chung, D.B. Chrisey, P.C. Dorsey, P. Matthews, A. Pique, T.E. Mlsna and J.L. Stepnowski, *IEEE Trans. Ultrason., Ferroelec., & Freq. Contr.*, **45**, 1370 (1998).
[11] K. Miyano and Y.R. Shen, *Phys. Rev. A*, **15** 2471 (1977).
[12] S. Sato and H. Ueda, *Jpn. J. Appl. Phys.*, **20** 511 (1981).